In-depth characterization of CD24^{high}CD38^{high} transitional human B cells reveals different regulatory profiles

Quentin Simon, MSc,[a] Jacques-Olivier Pers, DDS, PhD,[a] Divi Cornec, MD,[a,b] Laëtitia Le Pottier, PhD,[a] Rizgar A. Mageed, PhD, FRCP, FRCPath,[c] and Sophie Hillion, PhD[a] *Brest, France, and London, United Kingdom*

Background: CD24^{high}CD38^{high} transitional B cells represent cells at a key stage in their developmental pathway. In addition, these B cells have been widely ascribed regulatory functions and involvement in the control of chronic inflammatory diseases. However, the phenotypic and functional overlap between these cells and regulatory B cells remains controversial.

Objective: In this study we wanted to explore the regulatory properties of CD24^{high}CD38^{high} human B cells.

Methods: We used multicolor flow cytometry in combination with bioinformatics and functional studies to show that CD24^{high}CD38^{high} B cells can be distinguished into multiple subsets with different regulatory functions.

Results: For the first time, the study reveals that human transitional B cells encompass not only transitional type 1 and type 2 B cells, as previously suggested, but also distinct anergic type 3 B cells, as well as IL-10–producing CD27^{+} transitional B cells. Interestingly, the latter 2 subsets differentially regulate CD4^{+} T-cell proliferation and polarization toward T_H1 effector cells. Additional analyses reveal that the percentage of type 3 B cells is reduced and the frequency of CD27^{+} transitional B cells is increased in patients with autoimmune diseases compared with those in matched healthy subjects.

Conclusion: This study provides evidence for the existence of different transitional B-cell subsets, each displaying unique phenotypic and regulatory functional profiles. Furthermore, the study indicates that altered distribution of transitional B-cell subsets highlights different regulatory defects in patients with different autoimmune diseases. (J Allergy Clin Immunol 2016;137:1577-84.)

Key words: *Transitional B cells, immune regulation, chronic inflammatory diseases, autoimmunity*

Abbreviations used

APC: Allophycocyanin
BCR: B-cell receptor
Breg: Regulatory B
FITC: Fluorescein isothiocyanate
FLOCK: Flow Clustering without K
HC: Healthy control subject
KO: Krome orange
MFI: Mean fluorescence intensity
MNC: Mononuclear cell
PB: Pacific Blue
PC5: Phycoerythrin linked to cyanin 5
PE: Phycoerythrin
PLCγ2: Phospholipase Cγ2
pSS: Primary Sjögren syndrome
SLE: Systemic lupus erythematosus
SPADE: Spanning-tree Progression Analysis of Density-normalized Events
T1: Type 1
T2: Type 2
T3: Type 3

Transitional B cells represent a central developmental stage in B-cell maturation, linking generation in the bone marrow with differentiation in the periphery. The classification of murine transitional B cells into distinct type 1 (T1) and type 2 (T2) subsets was based on the expression of CD23, CD21, and the developmental marker CD24.[1] Studies of human B cells confirmed and extended the identification of transitional B cells in mice.[2,3] Early studies suggested that transitional human B cells can be subdivided into 2 major subsets: immature T1 cells identified as CD24^{high}CD38^{high}CD19^{+}CD10^{high}CD21^{low}CD5^{+} cells and intermediate transitional cells (T2) identified as CD24^{high}CD38^{high}CD19^{+}CD10^{+}CD21^{+}CD5^{low} cells.

The almost concurrent discovery of regulatory B (Breg) cells drew interest toward potential links with transitional B cells because of phenotypic and functional similarities.

Breg cells were first reported to be IL-10–producing B cells in mice and termed B10 cells.[4] Although almost all human B cells have the capacity to produce IL-10, the available evidence indicates that the "most efficient" IL-10–producing B cells are Breg cells, which are similar to CD24^{high}CD38^{high} transitional B cells.[5,6] Furthermore, associations between CD24^{high}CD38^{high} B cells and immune regulation were noted in the favorable clinical outcome of patients with chronic inflammatory and autoimmune diseases.[7] Specific allergen immunotherapy drives suppression of IgE and promotion of IgG_4 production by Breg cells.[8] These observations led investigators to draw parallels

From [a]EA2216, INSERM ESPRI, ERI29, Université de Brest, and LabEx IGO, Brest; [b]the Rheumatology Department, CHRU Brest Morvan; and [c]the William Harvey Research Institute, Queen Mary University of London.

Supported by the LabEX IGO program through investment of the future program ANR-11-LABX-0016-0.

Disclosure of potential conflict of interest: Q. Simon has received a grant from "Investissement d'avenir" programme (ANR11-LABX-0016-01). The rest of the authors declare that they have no relevant conflicts of interest.

Received for publication December 12, 2014; revised September 8, 2015; accepted for publication September 15, 2015.

Available online October 31, 2015.

Corresponding author: Sophie Hillion, PhD, Laboratoire d'Immunologie, CHRU Brest, BP824, 29609 Brest, France. E-mail: sophie.hillion@univ-brest.fr.

0091-6749/$36.00

http://dx.doi.org/10.1016/j.jaci.2015.09.014

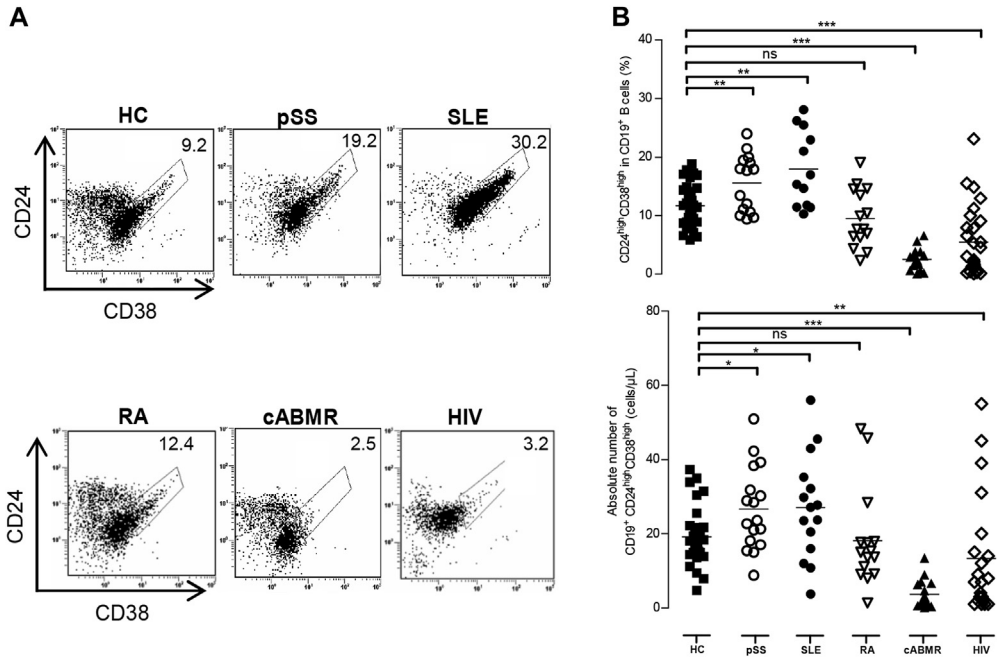

FIG 1. Comparison of $CD24^{high}CD38^{high}$ transitional B-cell subsets in patients and HCs. Blood from 33 HCs (■), 17 patients with pSS (○), 16 patients with SLE (●), 15 patients with rheumatoid arthritis (*RA*; ∇), 17 patients with chronic antibody-mediated rejection (*cABMR*; ▲), and 26 patients infected with HIV (◇) were analyzed by using flow cytometry. **A,** Representative *dot plots* of $CD24^{high}CD38^{high}$ cells in $CD19^{+}$ B cells. **B,** Percentages *(top panel)* and absolute numbers *(bottom panel)* of $CD19^{+}CD24^{high}CD38^{high}$ B cells in each group. $^{*}P < .05$, $^{**}P < .01$, and $^{***}P < .001$. *ns*, Not significant.

between $CD24^{high}CD38^{high}$ transitional B cells and Breg cells.[5,9-11] This in turn led to numerous studies and the emergence of differing theories about the relationship between transitional and "real" Breg cells.

To increase understanding of $CD24^{high}CD38^{high}$ transitional B cells and potential overlaps with Breg cells in human subjects, we developed a 10-color flow cytometric protocol for their phenotypic and functional characterization. The study reveals that $CD24^{high}CD38^{high}$ B cells incorporate phenotypically distinct B-cell subsets, each with distinct *in vitro* regulatory functions. Furthermore, the study reveals abnormal distribution of transitional B-cell subsets in patients with different autoimmune diseases, revealing new insights into Breg cell development and phenotype.

METHODS

Detailed procedures and standard methods used in the study are described in the Methods section in this article's Online Repository at www.jacionline.org.

Flow cytometry and cell sorting

All antibodies were purchased from Beckman Coulter (Fullerton, Calif) unless otherwise specified. All antibodies used to make up the 10-color panel are listed in Table E1 in this article's Online Repository at www.jacionline.org. Transitional B-cell subsets and $CD4^{+}$ T cells were sorted with MoFlow XDP (Dako–Beckman Coulter).

RESULTS

$CD24^{high}CD38^{high}$ B-cell frequency is variable in different diseases

High-level coexpression of CD24 and CD38 identifies circulating transitional human B cells and is often used by investigators for quantifying Breg cells in peripheral blood. We have observed that the frequency of $CD24^{high}CD38^{high}$ B cells varies in different clinical settings (Fig 1, *A*, and see Table E2 in this article's Online Repository at www.jacionline.org). The frequency and absolute number of $CD24^{high}CD38^{high}$ B cells in patients with primary Sjögren syndrome (pSS) and systemic lupus erythematosus (SLE) were significantly higher than in healthy control subjects (HCs; 15.5% ± 1.2% and 17.9% ± 1.8%, $P = .008$ and $P = .0037$, respectively; Fig 1, *B*).[12] Interestingly, during the active course of HIV infection, patients manifested a dramatic decrease in transitional B-cell percentages (5.3% ± 1.1% vs HCs, $P < 10^{-3}$). These observations suggest that it is difficult to universally associate decreases/increases in the frequency/number of $CD24^{high}$ $CD38^{high}$ B cells with pathophysiologic mechanisms.

Detailed characterization of $CD19^{+}CD24^{high}CD38^{high}$ B-cell subsets

To categorize $CD24^{high}CD38^{high}$ populations in B cells, we carried out a 10-color flow cytometric analysis using the Flow Clustering without K (FLOCK) software system.[13] First, we identified pregated transitional B cells, as defined by high expression levels of CD24 and CD38 in 2-dimensional plots within $CD19^{+}$ B cells (Fig 2, *A*). Next, we ran FLOCK software on compiled flow cytometric data from 15 independent experiments using isolated B cells from the HCs. This enabled us to identify 8 B-cell clusters within the $CD24^{high}CD38^{high}$ parent gate that partially overlapped in several biaxial box plots (Fig 2, *A*, and see Fig E1 in this article's Online Repository at www.jacionline.org). We observed that among the 10 chosen markers, CD27, IgM, and IgD were the best in differentiating B-cell

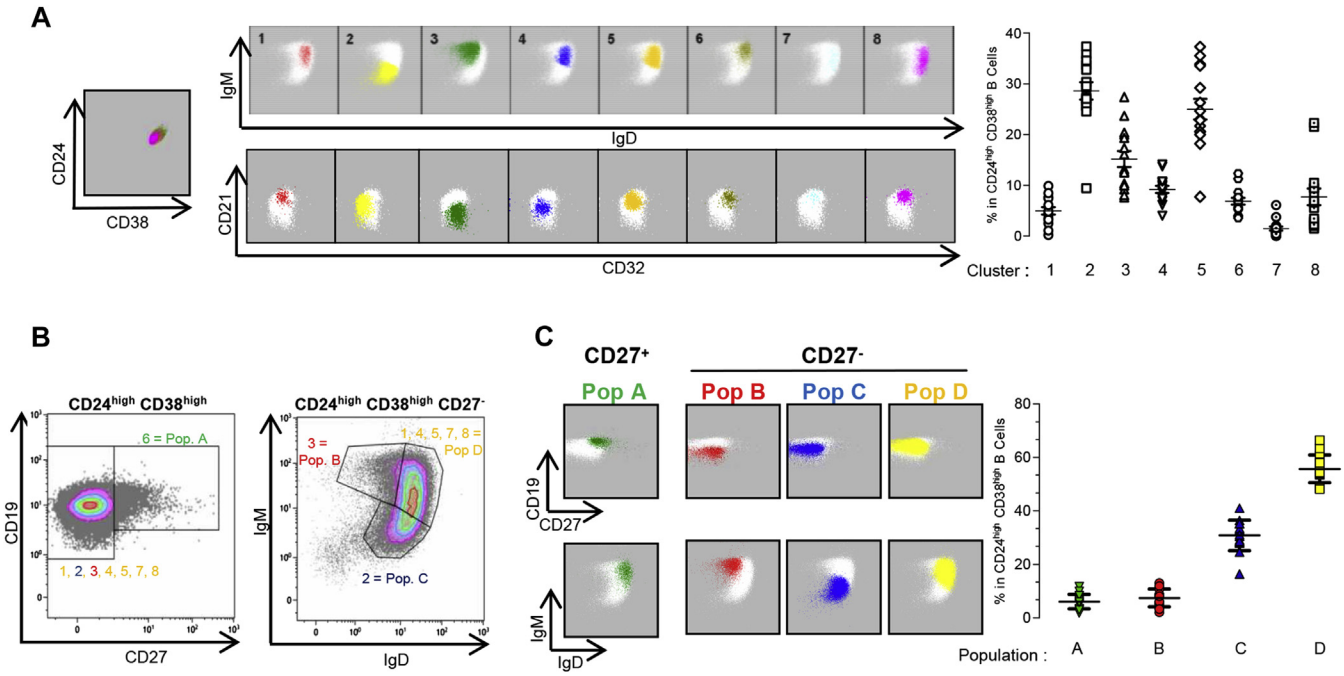

FIG 2. Identification and phenotypic definition of transitional B-cell subsets. **A,** Eight clusters of transitional B cells were identified by using FLOCK analysis. Representative *dot plots* of IgM/IgD and CD21/CD32 are shown in the *left panel*. The percentage of each cluster is depicted in the *right panel* as individual values in 15 HCs. **B,** The grouping strategy for classifying cell clusters is presented for CD19/CD27 and IgM/IgD expression. **C,** Supervised FLOCK analysis according to the previous grouping strategy and percentages of defined populations A, B, C, and D.

subsets within the 8 clusters based on mean fluorescence intensity (MFI; see Fig E2, *A*, in this article's Online Repository at www.jacionline.org). Cluster 6 displayed the highest MFI for CD27 expression (1639 ± 46.7; $P < 10^{-3}$). The MFI for IgM expression was higher in cluster 3 than in clusters 1 or 2 ($P < 10^{-3}$). Cluster 2 had a significantly reduced level of IgD and IgM expression. Analysis of other markers confirmed the noted distinctiveness of clusters 2 and 3 (see Fig E2, *A*). Consequently, we congregated the 8 clusters into 4 different patterns based on CD27, IgM, and IgD expression. Cluster 6 ($CD27^+$) was renamed population A. Cluster 3 ($IgD^{low}IgM^{high}$) was branded population B. Cluster 2 ($IgM^{low}IgD^{low}$) was named population C. Finally, we grouped clusters 1, 4, 5, 7, and 8, which expressed similar levels of IgM and IgD, into population D (Fig 2, *B*, and see Fig E2, *B* and *C*). Cross-sample comparison of these 4 populations was highly consistent between different blood donors (Fig 2, *C*). Populations C and D represented the majority of $CD24^{high}CD38^{high}$ B cells (55.7% ± 1.3% and 30.1% ± 1.5%, respectively).

Phenotypic characterization of transitional B-cell subsets identified by using FLOCK

We next carried out detailed phenotypic analysis of these 4 defined populations (Fig 3).

B-cell differentiation and activation markers. These analyses revealed that each cluster showed a unique B-cell profile of differentiation (Fig 3, *A*) and activation (Fig 3, *B*). Population A expressed CD27 and high levels of all of the other markers, with the exception of CD23, depicting a high activation status. Population B expressed lower levels of CD21, CD22, CD23, CD44, and CD62 ligand but had high levels of CD10 and CD32 (Fig 3, *A*). The results also revealed lower basal expression levels of HLA-DR, CD80, CD86, and CD25 in population C (Fig 3, *B*). These data suggest that population C might be in a resting state.

MitoTracker expression. The activity of the ATP-binding cassette transporter ABCB1 has been described as a functional characteristic that distinguishes transitional from mature naive B cells.[14] The level of MTG-Green MFI gradually decreased from population B to populations D and C, implying a developmental pathway through these subsets (see Fig E3, *A*, in this article's Online Repository at www.jacionline.org).

By compiling these descriptive data, the results provide evidence that population B presents a pattern of differentiation close to that seen in immature B cells, as described for T1 B cells (see Fig E3, *B*). Population D, in contrast, showed a progressive pattern of upregulating maturity markers in agreement with the previously defined T2 subset of B cells. Population C displayed an intermediate profile of activation markers consistent with what has been seen in a resting state described for type 3 (T3) B cells.[15] Finally, population A represents an atypically activated B cell with a memory-like phenotype, renamed $CD27^+$ transitional B cells (resumed in Fig E3, *B*).

Functional characteristics of T1, T2, T3, and $CD27^+$ transitional B-cell subsets

We next investigated functional characteristics of the transitional B-cell subsets.

Survival capacity. Reduced survival has been reported to be a functional characteristic of transitional B cells.[2] To compare and contrast this ability within the different subsets, we first analyzed

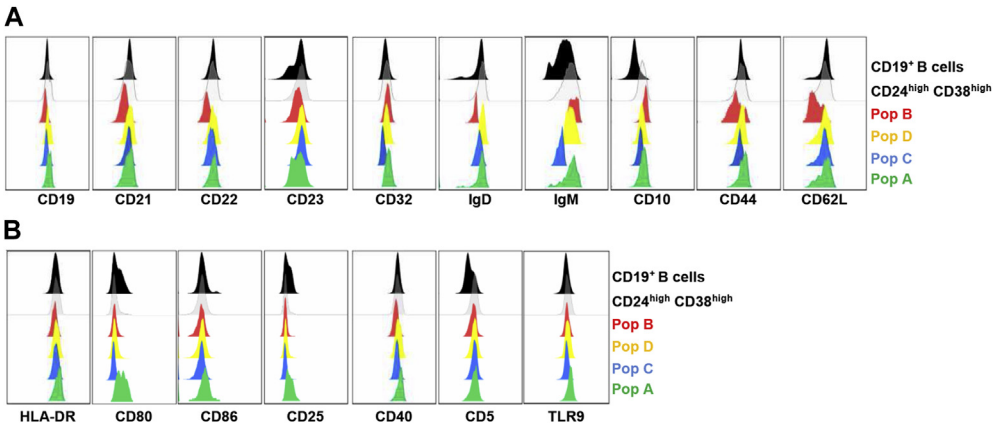

FIG 3. Broad phenotype of transitional $CD24^{high}CD38^{high}$ B-cell subsets. Representative histograms of surface markers are indicated for each gated population: $CD19^{+}$ B cells *(black)*, $CD19^{+}$ $CD24^{high}CD38^{high}$ cells *(gray)*, population A *(green)*, population B *(red)*, population C *(blue)*, and population D *(yellow)*. **A,** Expression of the differentiation markers. **B,** Expression of costimulatory and activation markers.

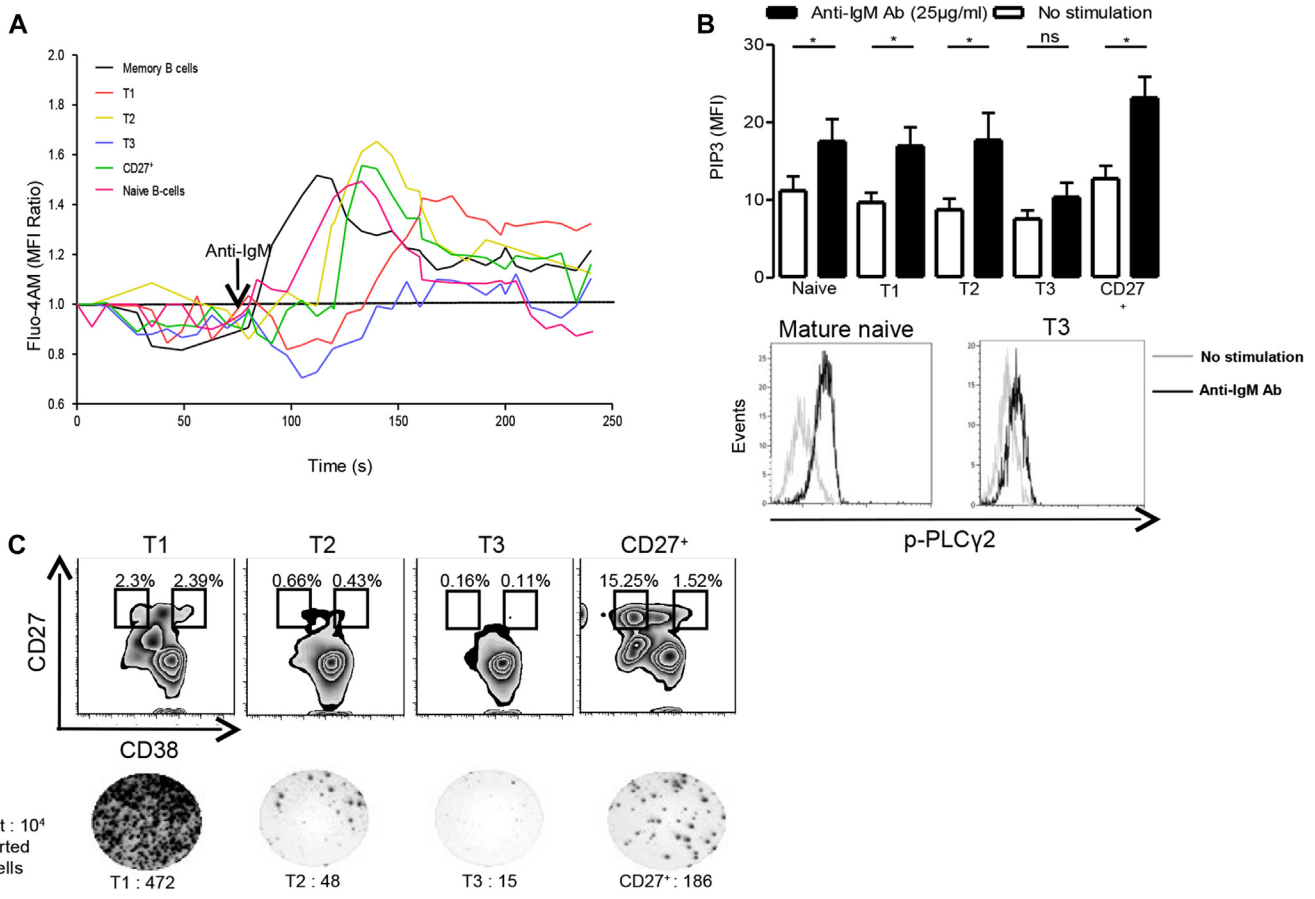

FIG 4. Transitional B-cell subsets respond differently to BCR and Toll-like receptor 9 engagements. **A,** Ca^{2+} flux after BCR engagement in different B-cell subsets. **B,** Intracellular staining for PIP3 *(top panel)* and phosphorylated p-PLCγ2 *(bottom panel)* levels after BCR engagement (n = 6). $*P < .05$. *ns,* Not significant. **C,** *In vitro* plasmablast differentiation and total IgM secretion (n = 3).

viability of the different $CD24^{high}CD38^{high}$ B-cell subsets in the absence of exogenous *stimuli* (see Fig E4 in this article's Online Repository at www.jacionline.org). The analysis revealed no significant differences between the subsets for early spontaneous apoptosis. We next studied whether B-cell receptor (BCR) engagement will modify survival of the transitional B-cell subsets. BCR engagement increased apoptosis in the T1 B-cell subset and did not increase survival in the other subsets (see Fig E4).

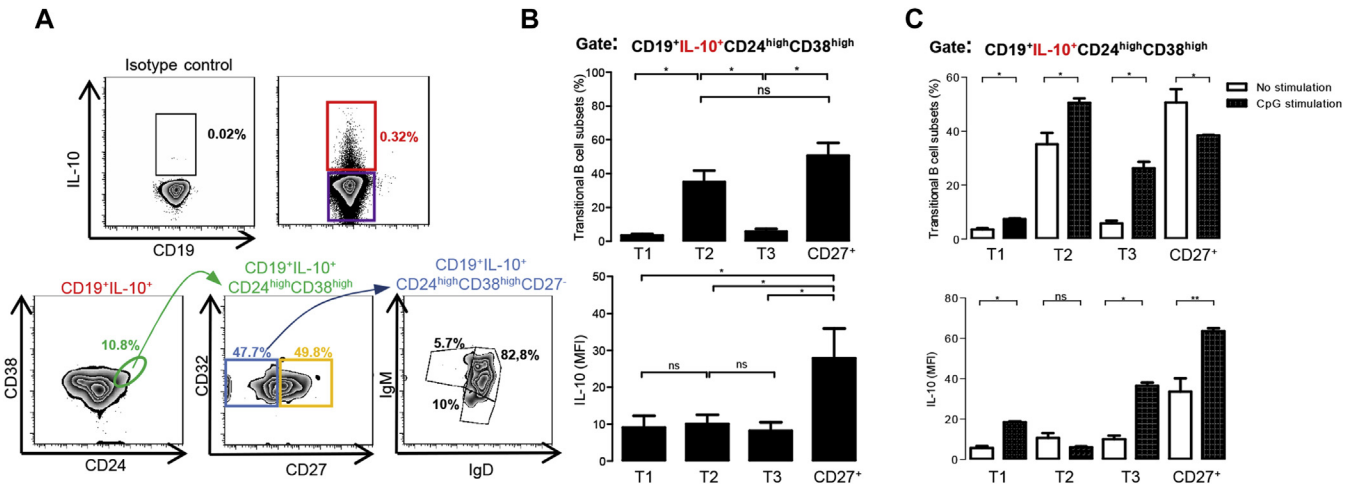

FIG 5. $CD27^+CD24^{high}CD38^{high}$ B cells are the most efficient spontaneous IL-10–producing transitional cells. **A,** Gating strategy used to evaluate IL-10 production by transitional B-cell subsets. **B,** Percentages of T1, T2, T3, and $CD27^+$ transitional B cells among $IL\text{-}10^+$ cells. *Bottom panel* depicts MFI for IL-10 in each transitional B-cell subset within $IL\text{-}10^+$ cells (n = 4). **C,** Comparison of mean ± SEM values of each transitional B-cell subset (and IL-10 MFI) in $IL\text{-}10^+CD24^{high}CD28^{high}$ B cells after 24 hours of stimulation with CpG-ODN (n = 4). $*P < .05$ and $**P < .01$. *ns,* Not significant.

Hyporesponsiveness of T3 B cells to BCR engagement. Low-density surface IgM is a hallmark of anergic B cells in mice and human subjects.[16] Such anergic B cells have been shown to be overrepresented among transitional B cells.[17] We next determined the functional response of the $CD24^{high}CD38^{high}$ B-cell subsets to BCR engagement. The ability of each subset to mobilize Ca^{2+} after BCR engagement was assessed by using flow cytometry.[18] BCR engagement induced similar increases in $[Ca^{2+}]$ influx in $CD27^+$ and T2 B cells (Fig 4, *A*). T3 B cells were unresponsive to BCR engagement, as indicated by a failure to mobilize Ca^{2+} on BCR activation.[16] To confirm this observation, we demonstrated that T3 B cells did not show an increase in PIP3 (phosphatidylinositol (3,4,5)-triphosphate) release (Fig 4, *B*, top panel) or increased phospholipase Cγ2 (PLCγ2) phosphorylation after BCR engagement (Fig 4, *B*, bottom panel).[19] These findings indicate that the T3 subset is refractory to BCR stimulation, which is consistent with a functional silencing similar to immunologic anergy.

T1 and $CD27^+$ transitional B cells provide innate humoral immunity. Transitional B cells are capable of contributing to innate humoral immunity by differentiating to polyreactive IgM antibody-producing cells.[20] Therefore we assessed whether differences existed between the transitional B-cell subsets in their ability to produce natural IgM antibodies. $CD24^{high}CD38^{high}$ B-cell subsets were sorted by means of flow cytometry (purity indicated in Fig E5, *A*) and incubated for 4 days with CpG-ODN (to mimic T cell–independent stimulation). B-cell differentiation was then analyzed by using flow cytometry (Fig 4, *C*). After 4 days of culture, $CD27^+$ transitional B cells differentiated significantly more to $CD27^+CD38^-$ memory B cells (15.2% ± 1.2%) than did T1 B cells (2.3% ± 0.4%). A very small number of T2 B cells acquired a memory phenotype (0.66% ± 0.1%), whereas almost none became $CD27^{high}CD38^{high}$ plasmablasts. T3 B cells did not differentiate on CpG stimulation.

We next analyzed the ability of the sorted transitional B-cell subsets to secrete natural IgM by using ELISpot (Fig 4, *C*, lower panel). Interestingly, T1 and $CD27^+$ transitional B cells showed a high capacity to differentiate into IgM-secreting cells. None of the populations switched antibodies from IgM to IgG or IgA (data not shown).

Regulatory functions of transitional B-cell subsets

IL-10 production. Previous studies have revealed that B-cell subsets producing IL-10 are consistently found within $CD24^{high}CD38^{high}$ and $CD24^{high}CD27^+$ cells.[5,21] To further determine the functional characteristics of transitional B-cell subsets, we next studied spontaneous IL-10 production *in vitro* without stimulation (Fig 5). Using a successive gating strategy (Fig 5, *A*), we observed that IL-10–producing B cells were mainly enriched in the T2 and $CD27^+$ B-cell subsets (35.1% ± 6.6% and 50.7% ± 7.4% of $IL\text{-}10^+$ B cells, respectively; Fig 5, *B*, and see Fig E6, *A* and *B*, in this article's Online Repository at www.jacionline.org). When the analysis was repeated with B cells stimulated through Toll-like receptor 9 for 24 hours, there was a dramatic increase in $IL\text{-}10^+$ B-cell counts within the T2 and T3 subsets (Fig 5, *C*). Activation of the cells with CpG-ODN enhanced IL-10 expression (MFI) in the pre-existing $IL\text{-}10^+CD27^+$ transitional B cells (Fig 5, *C*, and see Fig E6 *C-E*). Finally, to objectively present the data, we used Spanning-tree Progression Analysis of Density-normalized Events (SPADE) software, which maps cells in a hierarchic tree (see Fig E6, *F*). The data confirmed that the $CD27^+$ and T2 transitional B-cell subsets were the most inherently competent cells in producing IL-10. Interestingly, the SPADE analysis revealed that IL-10 could also be produced by other B-cell subsets.

Transitional $CD27^+$ B cells inhibit TNF-α and IFN-γ production by T cells. The available evidence indicates that transitional human B cells were the most efficient subset of Breg cells in inhibiting TNF-α and IFN-γ production by T cells.[5] To determine which of the transitional B cells characterized in this study best manifests the ability to regulate cytokine production by T cells, we used a specially adapted *in vitro* model system.[12,22]

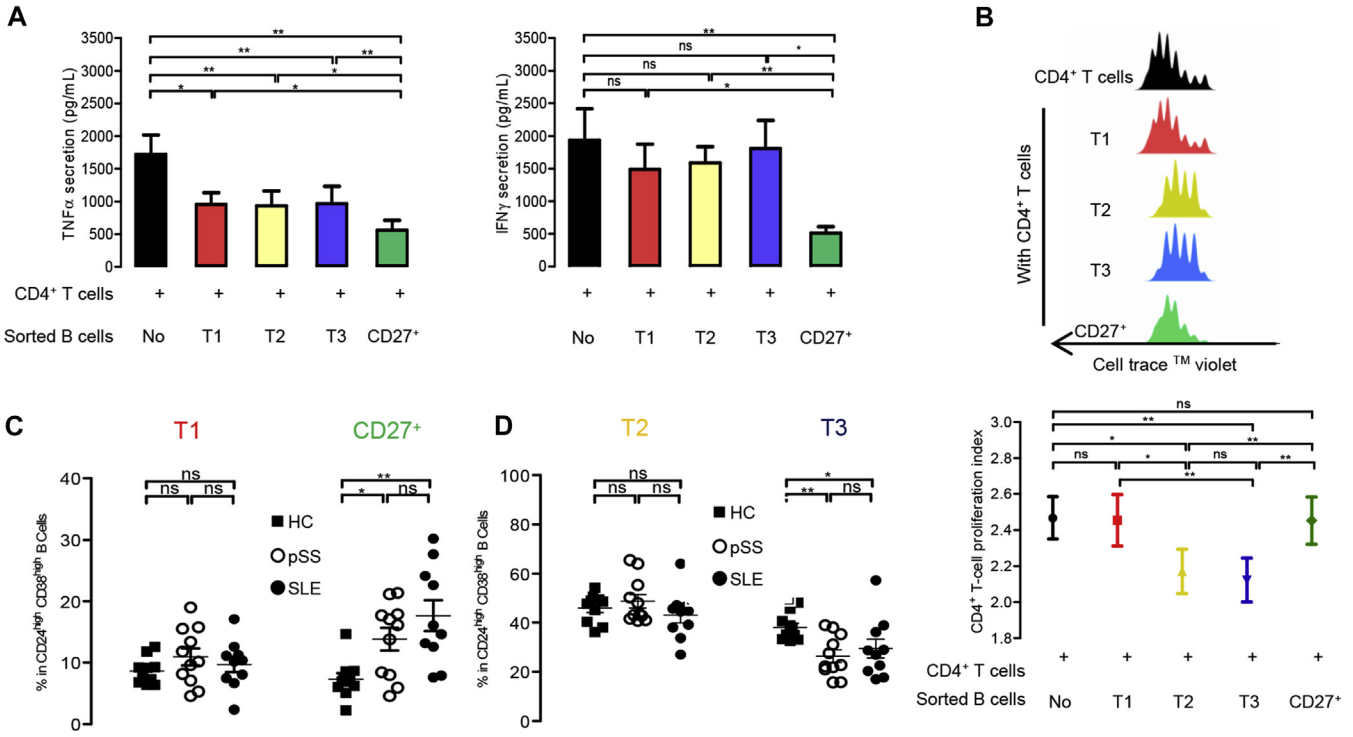

FIG 6. CD27$^+$ transitional B cells inhibit TNF-α and IFN-γ production by cultured T cells, whereas T3 B cells limit CD4$^+$ T-cell proliferation and are differentially represented in patients with different autoimmune diseases. **A,** Sorted CD4$^+$ T cells were cultured with each sorted transitional B-cell subset for 4 days. TNF-α and IFN-γ levels were measured in supernatants from cultured cells by using ELISA (n = 7). **B,** Representative histogram of CD4$^+$ proliferating T cells cultured with or without sorted transitional B-cell subsets *(top panel)*. Means ± SEMs of proliferation index of CD4$^+$ T cells in the presence or absence of transitional B-cell subsets (n = 10, *bottom panel*). **C,** Percentages of T1 and CD27$^+$ transitional B-cell subsets within CD24^{high}CD38^{high} B cells in HCs (■, n = 9), patients with pSS (○, n = 11), and patients with SLE (●, n = 10) after FLOCK cross-sample comparison. **D,** Percentages of T2 and T3 B-cell subsets. **P* < .05 and ***P* < .01. *ns*, Not significant.

The transitional B-cell subsets were fluorescence-activated cell sorted (purity >98%, as depicted in Fig E5, *A*) and cocultured with anti-CD3 and anti-CD28 antibody–activated CD4$^+$ T cells (purity >99% shown in Fig E5, *B*). All transitional B-cell subsets were able to reduce TNF-α production by CD4$^+$ T cells, but the CD27$^+$ B-cell subset was the most efficient ($P = .015$ vs T1 B cells, $P = .015$ vs T2 B cells, and $P = .0078$ vs T3 B cells; Fig 6, *A*). Interestingly, CD27$^+$ transitional B cells were the only subset within transitional B cells capable of significantly suppressing both TNF-α and IFN-γ production by CD4$^+$ T cells ($P = .0078$).

Anergic-like T3 B cells regulate T-cell proliferation. In the next set of experiments, proliferation of sorted CD4$^+$ T cells was studied by using flow cytometry at day 4 in the presence or absence of sorted transitional B-cell subsets (Fig 6, *B*). T1 and CD27$^+$ transitional B cells were unable to suppress T-cell proliferation. In contrast, T2 and T3 cells exhibited a significant ability to reduce CD4$^+$ T-cell proliferation. Interestingly, the T3 B-cell subset showed the highest reproducibility ($P = .0078$) in the ability to reduce T-cell proliferation among different donors when compared with T2 B cells ($P = .027$), suggesting that the latter might be composed of different functional subsets.

These observations demonstrate that transitional B-cell subsets have differential abilities to regulate T-cell responses.

Altered distribution of transitional B-cell subsets in patients with different autoimmune diseases. Finally, we investigated the distribution of each of the transitional B-cell subsets in patients with these autoimmune diseases. We performed a FLOCK cross-sample comparison of 10-color flow cytometric data on enriched B cells from 10 HCs, 11 patients with pSS, and 10 patients with SLE (Fig 6, *C* and *D*). The results showed that the frequency of CD27$^+$ transitional B cells was significantly increased in patients with pSS and SLE compared with that in HCs ($P = .03$ and $P = .0011$, respectively; Fig 6, *C*). Interestingly, the frequency of T3 B cells was decreased in patients compared with HCs ($P = .006$ in pSS patients and $P = .028$ in patients with SLE; Fig 6, *D*), whereas T1 and T2 B-cell frequencies were similar. These findings suggest that T3 and CD27$^+$ transitional B cells might have been influenced by a breach in peripheral tolerance in these patients.

DISCUSSION

Phenotypic and functional features of transitional B cells have been extensively studied in mice, leading to a qualified consensus that at least 3 major subsets of these cells exist.[1,15,17] However, in human subjects the biology of transitional B cells remains controversial. T1 and T2 subsets have consistently been identified within CD24^{high}CD38^{high} B cells.[23] In contrast, T3 B cells have

been suggested to be part of the mature B-cell pool.[3,14] In the current study we identified the T1 and T2 subsets by their differential capacity to survive or undergo apoptosis with BCR engagement.[24] However, our study provides new evidence for the existence of 2 additional transitional B-cell subsets with distinct phenotypic and functional properties. One subset, T3 B cells, expressed low levels of IgM, IgD, and CD10 and displayed functional status similar to anergic cells. Cells of the second subset, which includes $CD27^+$ transitional B cells, have not been described before as transitional B cells. Furthermore, these cells responded rapidly to T cell–independent stimuli and secreted natural IgM antibodies consistent with innate-like B cells.[25] In mice recent studies indicate that some transitional B cells have the potential to differentiate into plasmablasts and natural memory B cells.[26,27] Based on the findings made in the study, we developed a new paradigm (see Fig E6 in this article's Online Repository at www.jacionline.org) that includes a novel developmental pathway for transitional B-cell maturation in human subjects.

As a corollary to our hypothesis, we demonstrate that transitional B-cell subsets identified within the $CD24^{high}CD38^{high}$ B cells display differential regulatory abilities. Thus we reveal that $CD27^+$ transitional B cells are specialized in suppressing production of proinflammatory cytokines and have the capacity to produce high levels of IL-10 (Fig 5 and see Fig E6). Although the ability to produce IL-10 is often used as a marker of human Breg cells, we show that this is a property that is not restricted to a specific B-cell subset. Indeed, our analyses revealed that IL-10 can be produced by transitional B-cell subsets by $CD27^+CD24^{high}$ cells[21] and IgM^+IgD^- memory B cells (see Fig E6, *F*).[28] Furthermore, our data are consistent with studies of B cells in mice showing that B10 progenitor and effector cells can coexist in human transitional B cells.[21,29] Interestingly, T3 anergic-like B cells possessed the best and most consistent ability to control T-cell proliferation. The inconsistent suppressive ability of T2 B cells suggested that this subset might be heterogeneous.[30] The precise mechanism by which anergic B cells exhibit potent regulatory activities remains to be fully defined. The lack of costimulatory molecules (Fig 3 and see Fig E3) on the anergic-like B cells could induce anergy in the corresponding antigen-specific T cells.[31] Relevant to this observation, a recent study demonstrated that Ars/A1 anergic B cells are potent suppressors of humoral immunity in an IL-10–independent manner.[32]

These observations cast new light on existing but rather conflicting data on the phenotype of Breg cells by underlying the differential ability of different B-cell subsets to regulate distinct T-cell responses. Thus, for the first time, our study demonstrates that immune regulation by B cells is not confined to a "specific" B-cell subset and does not occur in a functionally restricted manner. Instead, the data show that different B-cell subsets can have different regulatory properties influenced by their microenvironment. In this regard a recent report suggested a developmental link between human transitional B cells and IL-10–producing plasmablasts.[27]

By using FLOCK cross-sample comparison analyses, the last part of our study revealed that patients with autoimmune diseases display abnormal distribution of transitional B-cell subsets. An increase in transitional B-cell counts in patients with SLE has been described before, but this did not correlate with disease activity.[2] Reduction in the frequency of T3 B-cell counts is consistent with the persistence of increased numbers of autoreactive mature B cells.[33] Furthermore, B cells from patients with SLE have been reported to be defective in their ability to suppress T-cell proliferation.[34] However, further investigation of transitional B-cell subsets would be required to accurately identify defective immune regulatory pathways in different diseases. Nevertheless, the study provides preliminary evidence that transitional B cells are not a homogeneous Breg cell population but rather represent a complex mixture of subsets from which different Breg cells emerge.[35] Thus the findings provide a new approach to define cellular biomarkers that identify specific defects in immune regulation in patients with different diseases.

We thank Simone Forest and Geneviève Michel for their secretarial assistance.

Clinical implication: Our study reveals that different human transitional B-cell subsets display different regulatory functions and that the frequency of such subsets is differentially altered in patients with different autoimmune diseases.

REFERENCES

1. Loder F, Mutschler B, Ray RJ, Paige CJ, Sideras P, Torres R, et al. B cell development in the spleen takes place in discrete steps and is determined by the quality of B cell receptor-derived signals. J Exp Med 1999;190:75-89.
2. Sims GP, Ettinger R, Shirota Y, Yarboro CH, Illei GG, Lipsky PE. Identification and characterization of circulating human transitional B cells. Blood 2005;105:4390-8.
3. Palanichamy A, Barnard J, Zheng B, Owen T, Quach T, Wei C, et al. Novel human transitional B cell populations revealed by B cell depletion therapy. J Immunol 2009;182:5982-93.
4. Fillatreau S, Sweenie CH, McGeachy MJ, Gray D, Anderton SM. B cells regulate autoimmunity by provision of IL-10. Nat Immunol 2002;3:944-50.
5. Blair PA, Norena LY, Flores-Borja F, Rawlings DJ, Isenberg DA, Ehrenstein MR, et al. CD19(+)CD24(hi)CD38(hi) B cells exhibit regulatory capacity in healthy individuals but are functionally impaired in systemic Lupus Erythematosus patients. Immunity 2010;32:129-40.
6. Bouaziz JD, Calbo S, Maho-Vaillant M, Saussine A, Bagot M, Bensussan A, et al. IL-10 produced by activated human B cells regulates CD4(+) T-cell activation in vitro. Eur J Immunol 2010;40:2686-91.
7. Anolik JH, Barnard J, Owen T, Zheng B, Kemshetti S, Looney RJ, et al. Delayed memory B cell recovery in peripheral blood and lymphoid tissue in systemic lupus erythematosus after B cell depletion therapy. Arthritis Rheum 2007;56:3044-56.
8. van de Veen W, Stanic B, Yaman G, Wawrzyniak M, Sollner S, Akdis DG, et al. IgG4 production is confined to human IL-10-producing regulatory B cells that suppress antigen-specific immune responses. J Allergy Clin Immunol 2013;131:1204-12.
9. Bao W, Zhong H, Manwani D, Vasovic L, Uehlinger J, Lee MT, et al. Regulatory B-cell compartment in transfused alloimmunized and non-alloimmunized patients with sickle cell disease. Am J Hematol 2013;88:736-40.
10. Duggal NA, Upton J, Phillips AC, Sapey E, Lord JM. An age-related numerical and functional deficit in CD19(+) CD24(hi) CD38(hi) B cells is associated with an increase in systemic autoimmunity. Aging Cell 2013;12:873-81.
11. Li X, Zhong H, Bao W, Boulad N, Evangelista J, Haider MA, et al. Defective regulatory B-cell compartment in patients with immune thrombocytopenia. Blood 2012;120:3318-25.
12. Nouel A, Segalen I, Jamin C, Doucet L, Caillard S, Renaudineau Y, et al. B cells display an abnormal distribution and an impaired suppressive function in patients with chronic antibody-mediated rejection. Kidney Int 2014;85:590-9.
13. Qian Y, Wei C, Eun-Hyung Lee F, Campbell J, Halliley J, Lee JA, et al. Elucidation of seventeen human peripheral blood B-cell subsets and quantification of the tetanus response using a density-based method for the automated identification of cell populations in multidimensional flow cytometry data. Cytometry B Clin Cytom 2010;78(suppl 1):S69-82.
14. Wirths S, Lanzavecchia A. ABCB1 transporter discriminates human resting naive B cells from cycling transitional and memory B cells. Eur J Immunol 2005;35:3433-41.
15. Allman D, Lindsley RC, DeMuth W, Rudd K, Shinton SA, Hardy RR. Resolution of three nonproliferative immature splenic B cell subsets reveals multiple

selection points during peripheral B cell maturation. J Immunol 2001;167: 6834-40.
16. Quach TD, Manjarrez-Orduno N, Adlowitz DG, Silver L, Yang H, Wei C, et al. Anergic responses characterize a large fraction of human autoreactive naive B cells expressing low levels of surface IgM. J Immunol 2011;186:4640-8.
17. Merrell KT, Benschop RJ, Gauld SB, Aviszus K, Decote-Ricardo D, Wysocki LJ, et al. Identification of anergic B cells within a wild-type repertoire. Immunity 2006; 25:953-62.
18. Seite JF, Goutsmedt C, Youinou P, Pers JO, Hillion S. Intravenous immunoglobulin induces a functional silencing program similar to anergy in human B cells. J Allergy Clin Immunol 2014;133:181-8, e1-9.
19. Browne CD, Del Nagro CJ, Cato MH, Dengler HS, Rickert RC. Suppression of phosphatidylinositol 3,4,5-trisphosphate production is a key determinant of B cell anergy. Immunity 2009;31:749-60.
20. Ueda Y, Liao D, Yang K, Patel A, Kelsoe G. T-independent activation-induced cytidine deaminase expression, class-switch recombination, and antibody production by immature/transitional 1 B cells. J Immunol 2007;178:3593-601.
21. Iwata Y, Matsushita T, Horikawa M, Dilillo DJ, Yanaba K, Venturi GM, et al. Characterization of a rare IL-10-competent B-cell subset in humans that parallels mouse regulatory B10 cells. Blood 2011;117:530-41.
22. Nouel A, Pochard P, Simon Q, Segalen I, Le Meur Y, Pers JO, et al. B-Cells induce regulatory T cells through TGF-beta/IDO production in A CTLA-4 dependent manner. J Autoimmun 2015;59:53-60.
23. Benitez A, Weldon AJ, Tatosyan L, Velkuru V, Lee S, Milford TA, et al. Differences in mouse and human nonmemory B cell pools. J Immunol 2014;192:4610-9.
24. Petro JB, Gerstein RM, Lowe J, Carter RS, Shinners N, Khan WN. Transitional type 1 and 2 B lymphocyte subsets are differentially responsive to antigen receptor signaling. J Biol Chem 2002;277:48009-19.
25. Genestier L, Taillardet M, Mondiere P, Gheit H, Bella C, Defrance T. TLR agonists selectively promote terminal plasma cell differentiation of B cell subsets specialized in thymus-independent responses. J Immunol 2007;178:7779-86.
26. Giltiay NV, Chappell CP, Sun X, Kolhatkar N, Teal TH, Wiedeman AE, et al. Overexpression of TLR7 promotes cell-intrinsic expansion and autoantibody production by transitional T1 B cells. J Exp Med 2013;210:2773-89.
27. Matsumoto M, Baba A, Yokota T, Nishikawa H, Ohkawa Y, Kayama H, et al. Interleukin-10-producing plasmablasts exert regulatory function in autoimmune inflammation. Immunity 2014;41:1040-51.
28. Khoder A, Sarvaria A, Alsuliman A, Chew C, Sekine T, Cooper N, et al. Regulatory B cells are enriched within the IgM memory and transitional subsets in healthy donors but are deficient in chronic GVHD. Blood 2014;124:2034-45.
29. Tedder TF. B10 cells: a functionally defined regulatory B cell subset. J Immunol 2015;194:1395-401.
30. Pillai S, Cariappa A, Moran ST. Marginal zone B cells. Annu Rev Immunol 2005; 23:161-96.
31. Dalai SK, Mirshahidi S, Morrot A, Zavala F, Sadegh-Nasseri S. Anergy in memory CD4+ T cells is induced by B cells. J Immunol 2008;181:3221-31.
32. Aviszus K, Macleod MK, Kirchenbaum GA, Detanico TO, Heiser RA, St Clair JB, et al. Antigen-specific suppression of humoral immunity by anergic Ars/A1 B cells. J Immunol 2012;189:4275-83.
33. Yurasov S, Wardemann H, Hammersen J, Tsuiji M, Meffre E, Pascual V, et al. Defective B cell tolerance checkpoints in systemic lupus erythematosus. J Exp Med 2005;201:703-11.
34. Lemoine S, Morva A, Youinou P, Jamin C. Human T cells induce their own regulation through activation of B cells. J Autoimmun 2011;36:228-38.
35. Rosser EC, Mauri C. Regulatory B cells: origin, phenotype, and function. Immunity 2015;42:607-12.

METHODS

Patients and control subjects

All patients and HCs provided informed consent, and the Ethics Committee at Brest University Medical School Hospital approved the study to be conducted in accordance with the Declaration of Helsinki Principles. Table E2 summarizes the characteristics of the patient groups included in the study.

Cell isolation

Mononuclear cells (MNCs) were isolated from peripheral blood by means of centrifugation on Ficoll-Hypaque. B cells were enriched from the MNCs by using negative selection with a B-cell enrichment kit (STEMCELL Technologies, Vancouver, British Columbia, Canada). T cells were enriched from MNCs by means of rosetting. All preparations were greater than 97% for B cells ($CD19^+$) or greater than 98% for $CD19^-CD5^+$ T cells.

Flow cytometry and cell sorting

All antibodies were purchased from Beckman Coulter, unless otherwise specified. The distribution of transitional B-cell subsets was determined by using fresh blood samples from patients and HCs. Briefly, 100 μL of peripheral blood collected in EDTA was mixed with PC7-conjugated anti-CD19 mAb (J3-119), phycoerythrin linked to cyanin 5 (PC5)–conjugated anti-CD38 mAb (L5198-4-3), and phycoerythrin (PE)–conjugated anti-CD24 mAb (ALB9) for 10 minutes at room temperature. Red blood cells were lysed with TQprep (Beckman Coulter).

Enriched B cells were stained with different combinations of fluorochrome-conjugated antibodies. All antibodies used to make up the 10-color panel are listed in Table E1. Additional staining included PE-conjugated anti-CD23 (8P25), PE–Texas Red–conjugated anti–CD62 ligand (DREG56), PC7-conjugated anti-HLA-DR (Imm-37), PE-conjugated anti-CD86 (HA5.2B7), PE-conjugated anti-CD40 (MAB89), Pacific Blue (PB)–conjugated anti-CD22 (SJ.10.1H11), PE-conjugated anti-CD44 (MEM.85), PE-conjugated anti-BR3 (T7.241), and/or PE-conjugated anti-TACI (1A1; BioLegend, San Diego, Calif) antibodies. In some experiments we used fluorescein isothiocyanate (FITC)–conjugated anti-CD80 (MAB104) antibody, FITC-conjugated rabbit anti-BCMA antibody (R&D Systems, Minneapolis, Minn), or FITC-conjugated anti-CD25 (2A3) mAb (BD Biosciences, San Jose, Calif) in combination with the 10-color panel. In addition, PB-conjugated anti-IgM (SAD4) antibody was used for some experiments. For ABCB1 transporter activity analysis, B cells were incubated with Krome orange (KO)–conjugated anti-CD19 antibody, APC Alexa Fluor-750-conjugated anti-CD24, PC5.5-conjugated anti-CD38, PC7-conjugated anti-CD27, allophycocyanin (APC)–conjugated anti-IgD, and PB-conjugated anti-IgM antibodies at 4°C for 30 minutes. Cells were then washed and incubated at 37°C for 30 minutes with 200 nmol/L MitoTracker Green FM probes (Molecular Probes, Eugene, Ore). Samples were acquired with a Navios cytometer (Beckman Coulter).

For BCR stimulation, enriched B cells were incubated with 25 μg/mL goat $(Fab')_2$ anti-human IgM antibody (Jackson Laboratories, Bar Harbor, Me) for 30 minutes at 4°C, followed by incubation for 5 minutes at 37°C. Cells were then fixed and permeabilized in 70% cold methanol for 30 minutes. Phosphatidylinositol (3,4,5)-trisphosphate production and PLCγ2 levels were measured by using flow cytometry with FITC-conjugated mouse anti-PIP3 antibody (Echelon, Salt Lake City, Utah) and PE-conjugated anti-PLCγ2 antibody (BD Biosciences).

Transitional B-cell subsets and $CD4^+$ T cells were sorted with MoFlow XDP (Dako–Beckman Coulter). The purity of B-cell subsets and T cells was greater than 98%.

Calcium influx

For intracellular calcium mobilization measurements, 2×10^5 B cells were stained with PC5.5-conjugated anti-CD38, AAF750-conjugated anti-CD24, PC7-conjugated anti-CD27, APC-conjugated anti-IgD, and KO-conjugated anti-CD32 mAbs at 4°C for 30 minutes. Cells were then washed and incubated at room temperature for 5 minutes with 2.5 mmol/L probenecid (Sigma-Aldrich, St Louis, Mo). Then 3 μmol/L Fluo-4 AM probe (Molecular Probes) in 0.02% pluronic-127 (FluoProbes; Interchim, Montlucon, France) prepared in HBSS plus 1% fetal bovine serum was added. The cells were maintained for 30 minutes at 30°C, washed, and analyzed at 37°C by using flow cytometry. After establishing the baseline for 30 seconds, the cells were stimulated with 25 μg/mL $(Fab')_2$ goat anti-IgM antibody. MFI was monitored for 5 minutes. The Fluo-4AM MFI ratio was calculated by using Fluo4-AM MFI for anti-IgM antibody–stimulated cells on a baseline of Fluo4-AM MFI for unstimulated cells from each subset.[E1]

Measurement of apoptosis

For apoptosis/necrosis assessment, 2×10^5 enriched B cells were cultured for 8 hours in medium alone or in the presence of 25 μg/mL $(Fab')_2$ goat anti-IgM antibody. Cells were stained with FITC-conjugated anti-CD19 (J3-119), PE-conjugated anti-CD24, PC5.5-conjugated anti-CD38, APC-conjugated anti-IgD, and KO-conjugated anti-CD22 mAbs and AAF-750-conjugated Draq7 Dye (Beckman Coulter). The cells were then washed and labeled with PB-conjugated Annexin V by using an apoptosis detection kit, according to the manufacturer's instructions (Beckman Coulter).

ELISA

Commercial ELISA kits with paired antibodies were used to measure IFN-γ and TNF-α levels (Beckman Coulter) in culture supernatants. Both ELISAs were performed according to the manufacturer's instructions.

In vitro B-cell differentiation and antibody production measurement by means of ELISpot

Sorted cells (10^4) from each transitional B-cell subset were activated in culture with 0.25 μmol/L CpG-ODN (2006) for 4 days. Differentiation of B cells to plasmablasts and memory cells was assessed by means of flow cytometry with FITC-conjugated anti-IgM antibody, PC7-conjugated anti-CD19 antibody, PE-conjugated anti-CD27 antibody, and PC5.5-conjugated anti-CD38 antibody. The level of total IgM production after plasmablast differentiation was studied by using the IgM ELISpotPLUS detection kit (MABTECH, Cincinnati, Ohio), according to the manufacturer's instructions. IgM-secreting cells were identified with an ELISpot reader.

IL-10 production assay

IL-10 measurement was carried out with an IL-10 secretion assay, according to the manufacturer's instructions (Miltenyi Biotec, Bergisch Gladbach, Germany). Briefly, 10^6 purified B cells were labeled with IL-10 catch reagent (or isotype) for 5 minutes on ice and then incubated in medium at 37°C for 45 minutes with continuous mixing. After the secretion period, the cells were washed and incubated with PE-conjugated IL-10 detection mAbs or PE-conjugated mouse IgG_1 as an isotype control counterstained with the mAbs listed in Table E1, except for CD10 and CD21.

Cell culture and proliferation assays

Sorted transitional B cells and $CD4^+$ T cells were cocultured for 4 days in RPMI-1640 complete medium, as previously described.[E2] For proliferation assays, sorted $CD4^+$ T cells were labeled with CellTrace Violet reagent (Molecular Probes) before coculture. T-cell proliferation was evaluated by using flow cytometry with the cell proliferation index in FlowJo software (FlowJo, Ashland, Ore).

Bioinformatic analyses and software

Bioinformatic analyses were performed with FLOCK. Files for each subject were uploaded to ImmPort (National Institutes of Health

Web site: www.immport.org) and analyzed by using FLOCK 1.0 to identify centroids for representative clusters. Markers listed in Table E1 were used. SPADE analysis was carried out by using the Cytobank platform.

Statistics

All data are expressed as means ± SEMs. Statistical analyses were performed with GraphPad Prism version 5.03 (GraphPad Software, La Jolla, Calif). The nonparametric Mann-Whitney *U* test or Wilcoxon *t* test for paired observations was used, and data were considered significant at a *P* value of less than .05.

REFERENCES

E1. Seite JF, Goutsmedt C, Youinou P, Pers JO, Hillion S. Intravenous immunoglobulin induces a functional silencing program similar to anergy in human B cells. J Allergy Clin Immunol 2014;133:181-8, e1-9.

E2. Nouel A, Pochard P, Simon Q, Segalen I, Le Meur Y, Pers JO, et al. B-Cells induce regulatory T cells through TGF-beta/IDO production in A CTLA-4 dependent manner. J Autoimmun 2015;59:53-60.

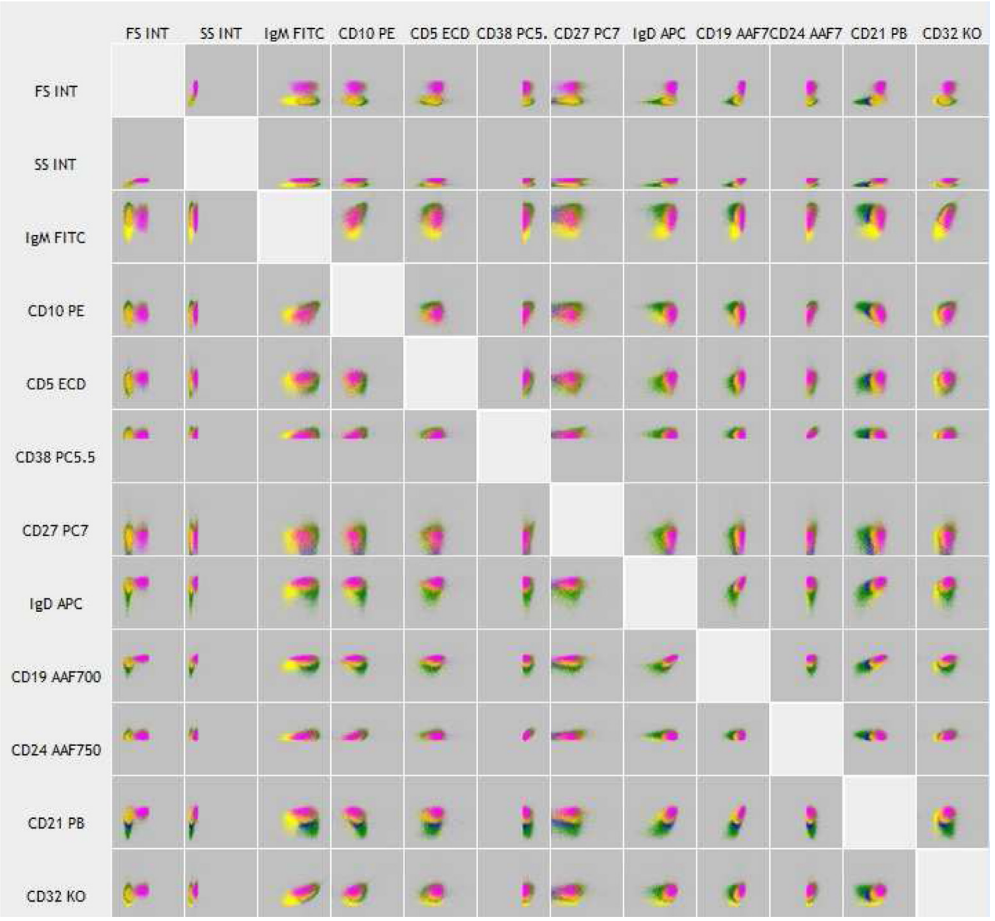

FIG E1. Event clusters identified by means of FLOCK analysis. FLOCK version 1.0 was run unsupervised on human B cells enriched from 15 HCs, stained with the 10-color B-cell panel of antibodies (Table E1), and pregated on $CD19^{+}CD24^{high}CD38^{high}$ lymphoid events. Overlay of the 8 identified clusters indicated in colors with percentages is shown in 1 representative HC as 2-dimensional plots.

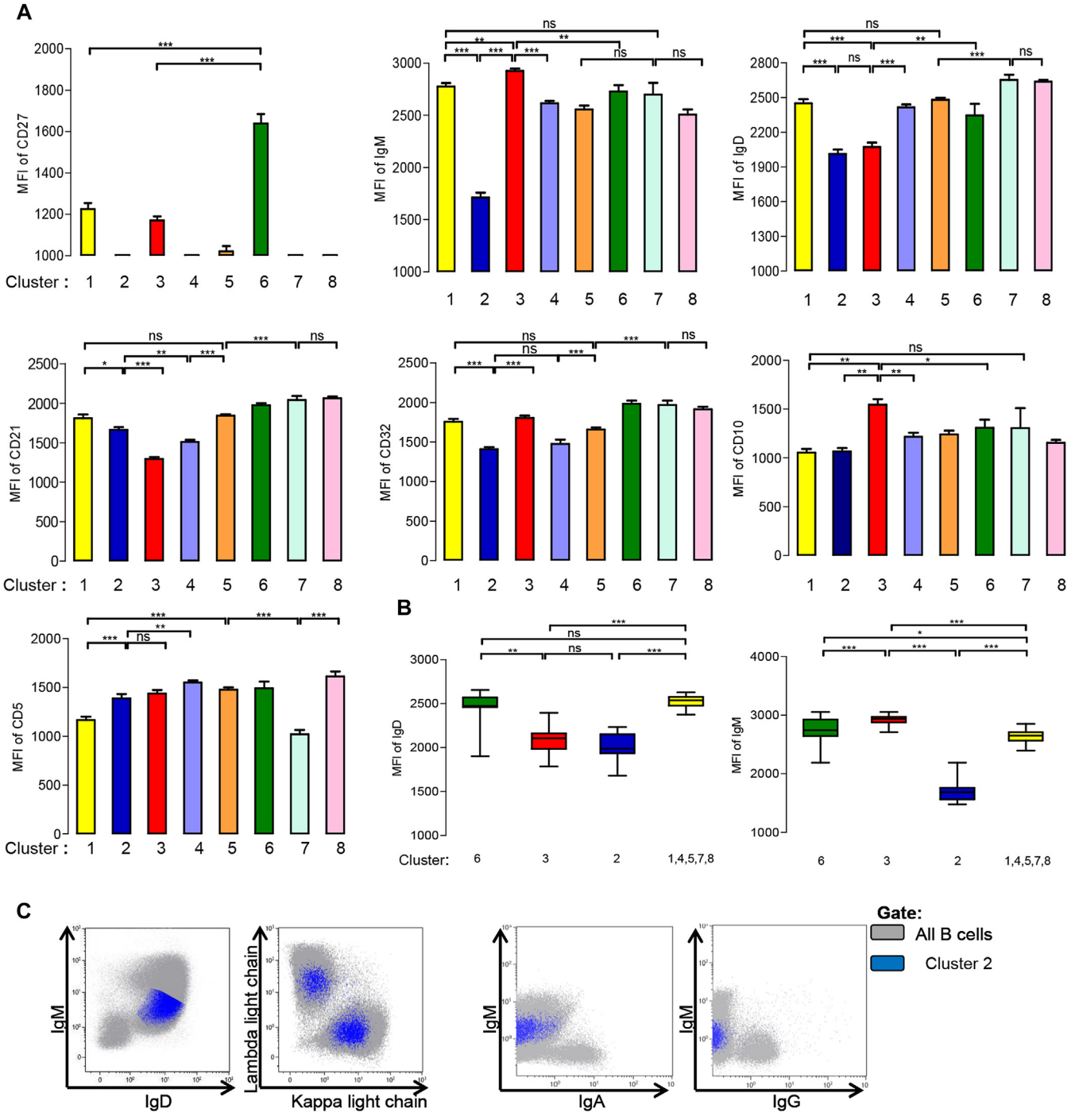

FIG E2. Determination of transitional B-cell populations. **A,** Means ± SEMs of MFIs for CD27, IgM, IgD *(top panel)*, CD21, CD32, CD10, and CD5 (*middle* and *bottom panels*). **B,** Means ± SEMs of IgM/IgD MFI identified by using Flock analysis and used for classifying cell clusters (n = 15). **P* < .05, ***P* < .01, and ****P* < .001. *ns*, Not significant. **C,** Kappa, lambda, IgA, and IgG expression on population C *(blue)* compared with whole B cells *(gray)*.

A

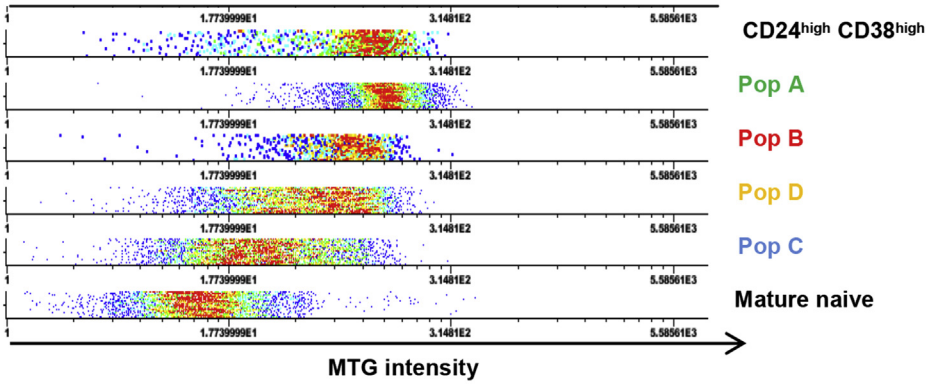

B

Population	Phenotype		B-cell subset
Pop A	$CD19^{++}$, $CD80^{++}$, $CD86^{++}$, $CD25^{++}$ and $CD40^{++}$ No ABCB1 transporter activity (MTG^{++})	Activated memory	$CD27^{+}$ transitional
Pop B	$CD10^{++}$, IgM^{++}, IgD^{low}, $CD32^{+}$ $CD21^{low}$, $CD44^{low}$, $CD62L^{low}$ and MTG^{+}	Immature	T1
Pop D	$CD10^{+}$, IgM^{+}, IgD^{+}, $CD32^{+}$, $CD21^{++}$, $CD23^{++}$ and MTG^{+}	Intermediate	T2
Pop C	$CD10^{low}$, IgM^{low}, IgD^{low}, $CD32^{low}$, $CD40^{low}$, HLA-DR^{low} and MTG^{low}	Resting state	T3

FIG E3. Phenotype of transitional $CD24^{high}CD38^{high}$ B-cell subsets. **A,** ABCB1 transporter activity. Mature naive B cells were identified as $CD19^{+}IgD^{+}CD27^{-}$ cells. **B,** Summary table indicating subset and population classification principles of transitional B cells and expression levels of the different markers.

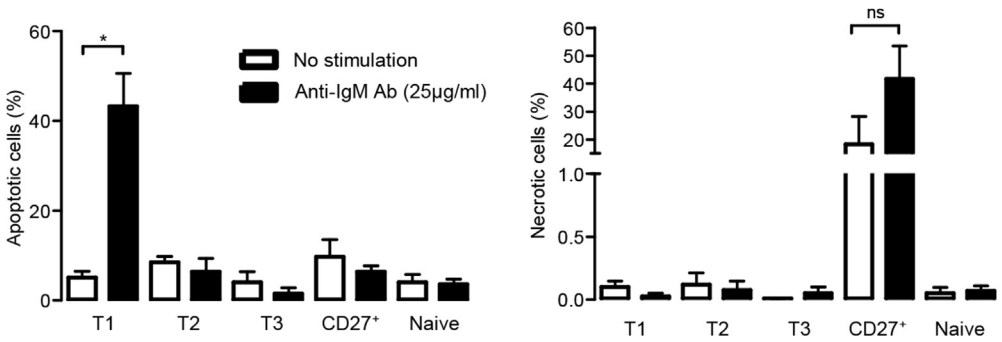

FIG E4. BCR engagement induces apoptosis in T1 B cells, whereas $CD27^+$ transitional B cells are prone to die in culture by means of necrosis. Percentages of apoptotic (Annexin V^+Draq7^-) and necrotic (Annexin V^+Draq7^+) cells are shown with and without BCR engagement for 8 hours (n = 4). *$P < .05$. *ns*, Not significant.

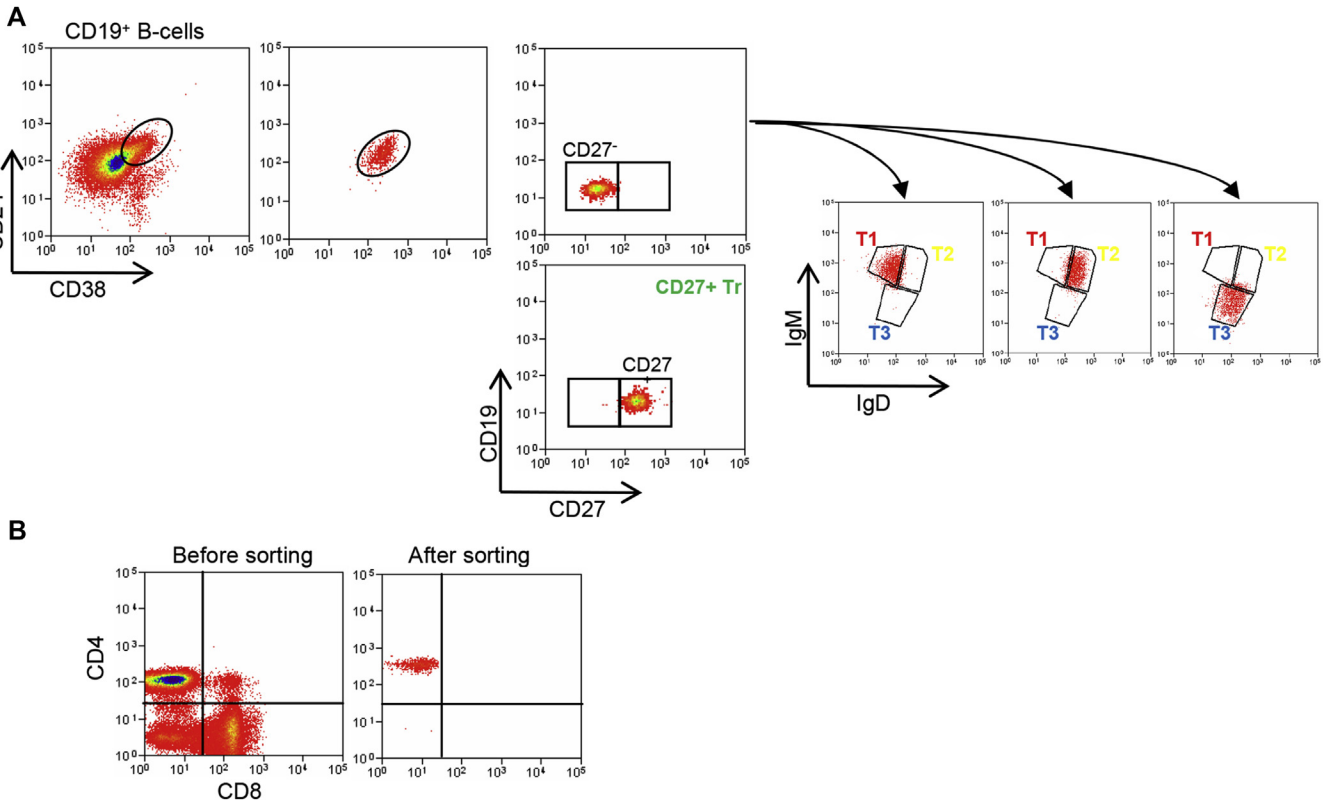

FIG E5. Purity of B- and T-cell subsets. **A,** Sorting strategy for enrichment of T1, T2, T3, and $CD27^+$ transitional B cells and purity of subsets after cell sorting are shown. **B,** $CD4^+$ T cells were sorted by means of flow cytometry from total T cells pre-enriched from PBMCs by means of rosetting.

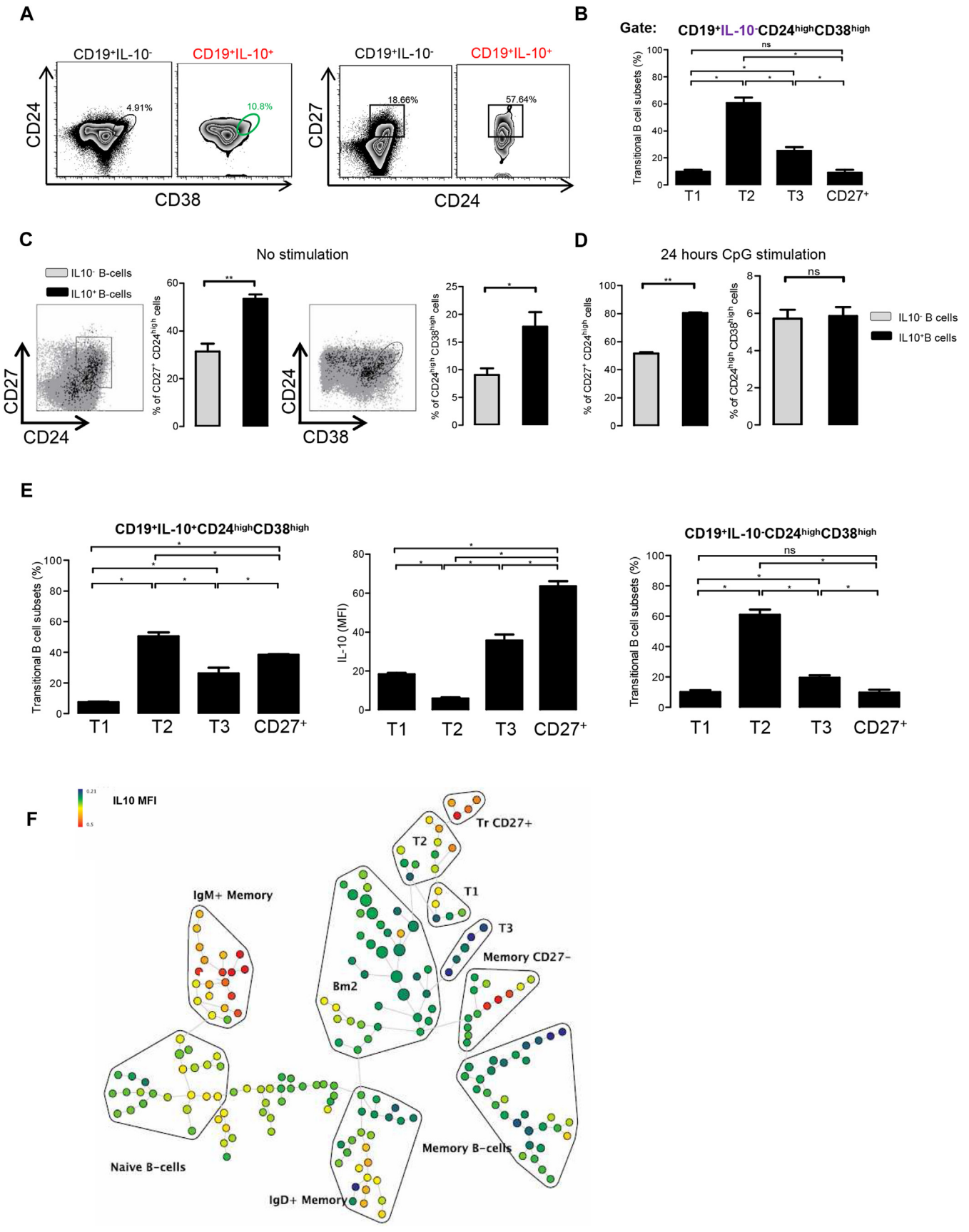
A
CD19+IL-10-
CD19+IL-10+
4.91%
10.8%
CD24
CD38
18.66%
57.64%
CD27
CD24
B
Gate: CD19+IL-10-CD24highCD38high
Transitional B cell subsets (%)
T1
T2
T3
CD27+
C
No stimulation
IL10- B-cells
IL10+ B-cells
% of CD27+ CD24high cells
% of CD24high CD38high cells
D
24 hours CpG stimulation
IL10- B cells
IL10+B cells
E
CD19+IL-10+CD24highCD38high
IL-10 (MFI)
CD19+IL-10-CD24highCD38high
F
IL10 MFI
Tr CD27+
IgM+ Memory
Bm2
Memory CD27-
Memory B-cells
Naive B-cells
IgD+ Memory

TABLE E1. List of fluorochrome-labeled antibodies used for the 10-color flow cytometric analysis

Specificity	Clone	Fluorochrome	Functions
CD19	J3-119	APC-AF700	Lineage
CD21	BL-13	PB	Signal transduction
CD32	2E1	KO	
CD10	ALB1	PE	B-cell growth
IgD	IA6-2	APC	Humoral response
IgM	SAD4	FITC	
CD27	1A4CD27	PE-Cy7	Memory
CD38	LS198-4-3	PE-Cy5.5	Proliferation
CD24	ALB9	APC-AF750	Proliferation
CD5	BL1a	ECD	Signal transduction, activation

ECD, PE–Texas Red.

FIG E6. IL-10 production by transitional B-cell subsets. **A,** CD24/CD38 and CD27/CD24 *dot plots* depicted on IL-10$^+$ and IL-10$^-$ B cells. **B,** Percentages of T1, T2, T3, and CD27$^+$ transitional B cells in IL-10$^-$ cells. **C,** Enriched B cells were stained with antibodies with specificity for CD19, CD24, CD38, and CD27 markers. IL-10 levels were measured by using an IL-10 secretion assay during 45 minutes. Means ± SEMs of CD27^{high}CD24^{high} and CD24^{high}CD38^{high} B cells in IL-10$^+$ and IL-10$^-$ B cells are shown. **D,** IL-10 production was measured after 24 hours of culture in the presence of CpG-ODN (2006; 0.25 μmol/L). Means ± SEMs of CD27^{high}CD24^{high} and CD24^{high}CD38^{high} B cells in IL-10$^+$ and IL-10$^-$ B cells are shown. **E,** Means ± SEMs of percentages of each transitional B-cell subset (and IL-10 MFI) in IL-10$^+$ and IL-10$^-$ CD24^{high}CD38^{high} B cells after stimulation of the cells with CpG-ODN. **F,** SPADE analysis of IL-10 density-based expression in all nonstimulated B-cell subsets. We derived annotations according to the differential pattern of expression of each marker previously chosen to differentiate the various transitional B-cell subsets: CD24, CD38, IgM, IgD, CD27, CD32, and CD19. *$P < .05$ and **$P < .01$. *ns*, Not significant.

TABLE E2. Characteristics of patients included in the study

Patients	Median age (y [range])	Sex ratio, female/male	Treatments
pSS (n = 17)*	56 (29-77)	17/0	CTC = 3, PLQ = 4
SLE (n = 16)†	41.5 (25-76)	14/2	CTC = 4, PLQ = 11, MPA = 1, MTX = 3, Thal. = 2
RA (n = 15)	51 (29-80)	8/7	CTC = 12, PLQ = 2, MTX = 10, RTX = 3, anti–IL-6 = 1, anti–TNF-α = 7
cABMR (n = 17)	54.5 (27-73)	3/14	CTC = 15/17, MPA = 17/17, mTORi = 2/17
HIV (n = 26)	50 (37-62)	8/16	Not informed

cABMR, Chronic antibody-mediated kidney graft rejection; *CTC*, corticosteroids; *MPA*, mycophenolic acid; *mTORi*, mammalian target of rapamycin inhibitor receptor; *MTX*, methotrexate; *PLQ*, Plaquenil; *RA*, rheumatoid arthritis; *RXT*, rituximab; *Thal.*, thalidomide.

*Eleven patients with pSS.

†10 patients with SLE were considered for the FLOCK cross-sample comparison (Fig 6).